

**Topotactic Reduction and Reoxidation of Hexagonal $\text{RCu}_{0.5}\text{Ti}_{0.5}\text{O}_3$ (R =Y, Eu-Lu)
Phases**

Peng Jiang, Romain Berthelot, Jun Li, A.W. Sleight, and M.A. Subramanian*

Department of Chemistry, Oregon State University, Corvallis, OR 97331-4003, USA

Email addresses of all authors:

Peng Jiang: jiangp@onid.orst.edu

Romain Berthelot: berthelot.rom@gmail.com

Jun Li: jli100@yahoo.com

A. W. Sleight: arthur.sleight@oregonstate.edu

M. A. Subramanian: mas.subramanian@oregonstate.edu

Telephone number for all the authors: 1-541-737-6750

Fax number for all the authors: 1-541-737-2062

Corresponding Author Permanent Address:

M. A. Subramanian

Department of Chemistry,

Oregon State University

153 Gilbert Hall

Corvallis, OR 97331 U.S.A.

1-541-737-8235 or 1-541-737-6750

Email: mas.subramanian@oregonstate.edu

Abstract

Hexagonal AMO_2 and AMO_3 phases have the same basic structure, and intermediate compositions for this structure have been prepared by topotactic oxidation of AMO_2 phases such as RCuO_2 , where R is a trivalent rare earth cation. We now find that such intermediate phases can also be prepared by topotactic reduction of hexagonal $\text{RCu}_{0.5}\text{Ti}_{0.5}\text{O}_3$ (R = Y, Tb-Lu) phases. Our TGA and magnetic susceptibility studies indicate a formula of $\text{RCu}_{0.5}\text{Ti}_{0.5}\text{O}_{2.78}$ for these reduced phases. Topotactic reoxidation occurs on heating these phases to 400°C in air.

KEYWORDS: A. Inorganic compounds, B. Chemical synthesis, D. Crystal Structure
Electronic properties, D. Magnetic Properties

1. Introduction

Two structurally related hexagonal AMO_2 and AMO_3 phases both have an uncommon coordination for the M cation (Fig. 1). The M cation in the AMO_2 phases (delafossite structure) is 2-fold linear; thus, the M cation is usually Cu^{1+} or Ag^{1+} . The M cation in the structurally related AMO_3 phases is trigonal bipyramidal, and M can be Fe, Mn, In, or Ga. The space group for the 2H form of the delafossite structure and the paraelectric form of hexagonal AMO_3 is $P6_3/mmc$, the only difference being the oxygen content. The O atom present in both the hexagonal AMO_2 and AMO_3 structure will be referred to as Oa (axial), and the O atom present only in the hexagonal AMO_3 structure will be referred to as Ob (basal plane). A structural variation can occur in both the hexagonal AMO_2 and the hexagonal AMO_3 structure. For the AMO_2 composition a commonly observed different stacking of the layers gives rise to the 3R polymorph, but this stacking sequence is unfavorable for the AMO_3 composition. Stacking sequences other than 2H and 3R can occur but are rare [1]. In the case of the hexagonal AMO_3 compounds, the extra oxygen relative to AMO_2 is usually underbonded, and this leads to a structural distortion and ferroelectricity [2].

As far as we are aware there has been no report of intergrowth of the hexagonal AMO_2 and AMO_3 structures. Also, there have apparently been no reports of compositions intermediate between hexagonal AMO_2 and AMO_3 prepared by direct synthesis. However, oxygen intercalation can occur if the A cation is at least as large as Sc. The oxidation of ScCuO_2 proceeds up to $\text{ScCuO}_{2.5}$ with complete oxidation of Cu^{1+} to Cu^{2+} [3]. The thermodynamically stable form of $\text{Sc}_2\text{Cu}_2\text{O}_5$ has a completely different structure. In the case of LaCuO_2 topotactic oxidation up to $\text{LaCuO}_{2.68}$ has been reported [4]. Double substitution into the M site of the hexagonal AMO_3 structure gives $\text{RCu}_{0.5}\text{Ti}_{0.5}\text{O}_3$ (R = Y, Tb-Lu) phases [5]. Solid solutions between $\text{YCu}_{0.5}\text{Ti}_{0.5}\text{O}_3$ and YMO_3 where M = Mn, Cr, Fe, Al, Ga and In have also been investigated [6].

2. Experimental

For the synthesis of the $\text{RCu}_{0.5}\text{Ti}_{0.5}\text{O}_3$ ($\text{R} = \text{Y, Tb-Lu}$) phases, stoichiometric mixtures of powders of rare earth oxides, CuO , and TiO_2 were ground together in an agate mortar, pelleted, and heated at 1050°C for 12 hours in air. Reagents were all at least 99.9% pure. Subsequently, the samples were heated under N_2 containing 5% H_2 at temperatures ranging from 150°C to 500°C for 4 hrs. X-ray diffraction patterns were obtained at room temperature with a Rigaku Miniflex diffractometer with $\text{Cu K}\alpha$ radiation and a graphite monochromator on the diffracted beam. Data were collected over a 2θ range of 10 - 95° with a step size of 0.02° with 2s at each step. Refinement of unit cell dimensions utilized fitting of the patterns by the Le Bail method with GSAS software.

Diffuse reflectance spectra of powdered samples were obtained in the region 300-1100 nm with a fiber optics system. In this method, light from a light source is passed through a bifurcated (Y-shaped) optical fiber assembly onto the sample, and back into the bifurcate optical fiber where it is taken to a spectrophotometer. BaSO_4 was served as a white reference. The data were transformed into absorbance with the Kubelka-Munk function.

Magnetic data were obtained on a Quantum Design, Physical Property Measuring System over a temperature range of 5 to 320 K. Data were collected with the zero field cooling method with an applied magnetic field of 0.5 T. Diamagnetic corrections were applied for all the samples measured [7]. The Curie and Weiss constants were derived from plots of $1/\chi$ versus T.

Thermogravimetric analysis was performed with a TA Instruments Q50 Thermogravimetric Analyzer. A reduced powder sample of $\text{YCu}_{0.5}\text{Ti}_{0.5}\text{O}_3$ was heated in oxygen at $10^\circ\text{C}/\text{min}$ ramp rate and held at 200°C and 400°C for 2h, respectively. The previous reduction of this sample was carried out at 200°C for 12h in 5% H_2/N_2 .

3. Results

For $\text{YCu}_{0.5}\text{Ti}_{0.5}\text{O}_3$ reduction treatments were conducted at 100, 150, 200, 250, 300, 400, and 500°C. The color and the XRD patterns remained unchanged after the 100 and 150°C treatments. However, the samples turned dark brown or black at treatment at higher temperatures, consistent with our diffuse reflectance spectra (Fig. 2). The XRD patterns (Fig. 3) also changed for the 200°C and higher temperature treatments. The peak positions shifted, the peaks broadened, and the weak peaks resulting from the ferroelectric distortion have disappeared. The peak broadening could be due to crystallite size reduction, inhomogeneity induced strain, or a combination of these two. The disappearance of the ferroelectric distortion is not surprising because it is driven by O_b displacements along the c axis, and the vacancies at the O_b site would disrupt the cooperative interactions necessary for such a transition. The XRD pattern of a sample treated at 500°C under our reducing conditions indicated sample decomposition.

The $\text{RCu}_{0.5}\text{Ti}_{0.5}\text{O}_3$ ($\text{R} = \text{Tb-Lu}$) phases were all subjected to the same reduction treatment at 400°C, and similar color and XRD pattern changes were observed. The unit cell information obtained before and after treatment is given in Fig. 4. For all the $\text{RCu}_{0.5}\text{Ti}_{0.5}\text{O}_3$ ($\text{R} = \text{Y, Tb-Lu}$) phases the reduction resulted in an increase in the a cell edge and a decrease in the c cell edge. In all cases the increase in unit cell volume on reduction is 3-4%.

Results of TGA reoxidation of a reduced $\text{YCu}_{0.5}\text{Ti}_{0.5}\text{O}_3$ phase are shown in figure 5. The weight gain of 1.82% indicates that the formula before this reoxidation was $\text{YCu}_{0.5}\text{Ti}_{0.5}\text{O}_{2.78}$. The XRD pattern changes very little during this topotactic reoxidation.

The dramatic drop in the magnetic susceptibility values on reduction of $\text{YCu}_{0.5}\text{Ti}_{0.5}\text{O}_3$ is shown in Fig. 6. Before reduction the magnetic susceptibility data for both $\text{YCu}_{0.5}\text{Ti}_{0.5}\text{O}_3$ and $\text{LuCu}_{0.5}\text{Ti}_{0.5}\text{O}_3$ gave a moment of 2.6 $\mu\text{B}/\text{Cu}$. The spin only value for Cu^{2+} is 1.73 μB , but experimental values for Cu^{2+} are usually higher and attributed to an orbital angular momentum contribution [8,9]. The moment observed

after reduction is reduced to 0.33 μB . Assuming that only Cu^{2+} is reduced and that the orbital angular momentum contribution remains the same, 13% of the Cu^{2+} has not been reduced and the composition would be $\text{YCu}_{0.5}\text{Ti}_{0.5}\text{O}_{2.78}$, in agreement with our TGA results.

Qualitative conductivity measurements were attempted at room temperature for all samples with the 2-probe method. The resistance was always too high to measure for the oxidized samples, indicating that they are electrical insulators. Resistivities as low as 1 $\Omega\text{-cm}$ were observed for reduced samples.

4. Discussion

The consistency of the degree of unit cell volume increase for all $\text{RCu}_{0.5}\text{Ti}_{0.5}\text{O}_3$ ($\text{R} = \text{Y}, \text{Tb-Lu}$) phases on reduction suggests a similar degree of reduction in all cases. This volume increase on reduction can be attributed to the fact cations always increase in size as they are reduced. The established redox behavior of Cu and Ti would indicate that the Cu^{2+} would oxidize Ti^{3+} to Ti^{4+} ; thus, we expect no Ti^{3+} in our reduced samples. The dark color of our reduced phases could be attributed to a Cu^{1+} - Cu^{2+} intervalence transition. However, both CuNbO_3 and CuTaO_3 are reported to be black [10], suggesting that the electron transfer from Cu^{1+} to d^0 cations such as Nb^{5+} , Ta^{5+} and Ti^{4+} may be of sufficiently low energy to contribute to this dark color.

Acknowledgement

The work is supported by a grant from National Science Foundation (DMR 0804167).

References

1. R. Berthelot, M. Pollet, J.-P. Doumerc, and C. Delmas *Inorg. Chem.*, 50 (2011) 4529.
2. A.W. Sleight, *Prog. Solid State Chem.* 37 (2009) 251.
3. J. Li, A. Yokochi, A.W. Sleight *Solid State Sci.* 6 (2004) 831.

4. R.J. Cava, H.W. Zandbergen, A.P. Ramirez, H. Takagi, C.T. Chen, J.J. Krajewski, W.F. Peck Jr. Jr., J.V. Waszczak, G. Meigs, R.S. Roth, L.F. Schneemeyer, *J. Solid State Chem.* 104 (1993) 437.
5. M. T. Anderson; K. B. Greenwood, G.A. Taylor, K.R. Poeppelmeier, *Prog. Solid. State. Chem.* 22, 197, 1993; N. Floros; J. T. Rijssenbeek; A. B. Martinson; K. R. Poeppelmeier. *Solid. State. Sci.* 4, (2002) 1495.
6. A. E. Smith, A. W. Sleight, M.A. Subramanian, *Mater. Res. Bul.* 46 (2011) 1.
7. G. A. Bain, J. F. Berry. *J. Chem. Edu.* 85 (2008) 532.
8. J. Lewis, *Science Progress*, 50 (1962) 419.
9. D. Choudhury, A. Hazarika, A. Venimadhav, C. Kakarla, K. T. Delaney, P. Sujatha Devi P. Mondal, R. Nirmala, J. Gopalakrishnan, N. A. Spaldin, U. V. Waghmare and D. D. Sarma, *Phy. Rev. B.* 82, (2010) 134203.
10. A.W. Sleight and C.T. Prewitt, *Mater. Res. Bull.*, 5 (1970) 207.

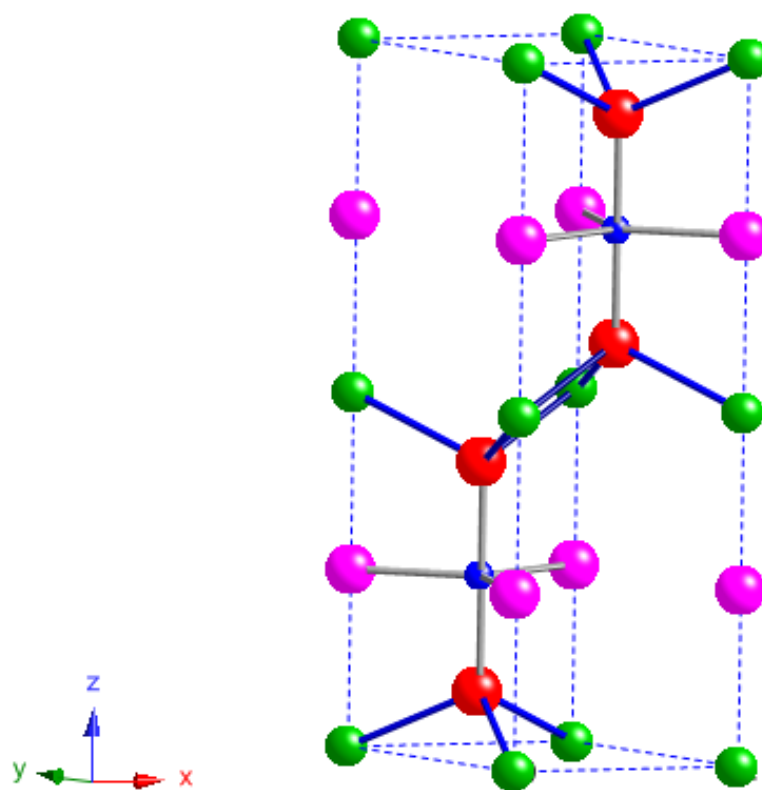


Figure 1. Structure for hexagonal RMO₂ and RMO₃ compounds where R is green, M is blue, O_a is red, and O_b is magenta. The O_b atoms are missing for the AMO₂ composition.

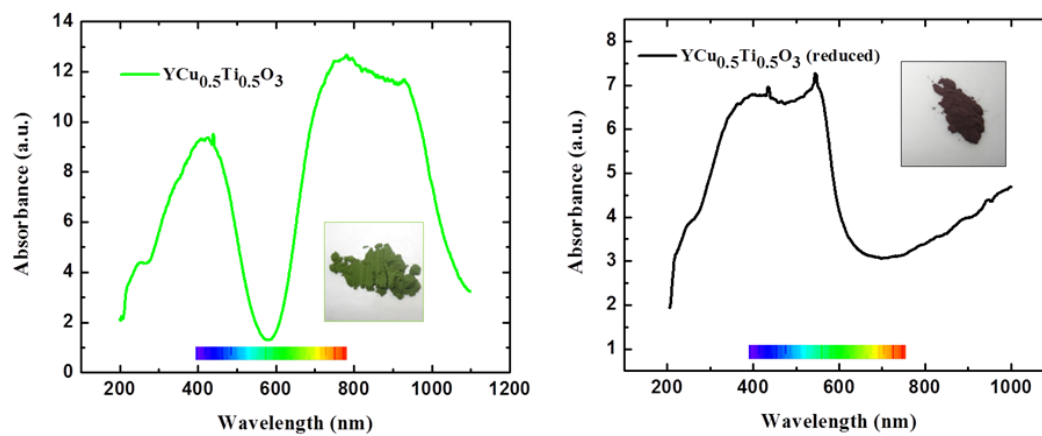


Figure 2. Diffuse reflectance spectra of $\text{YCu}_{0.5}\text{Ti}_{0.5}\text{O}_3$ as prepared (left) and reduced in H_2/N_2 gas mixture (right).

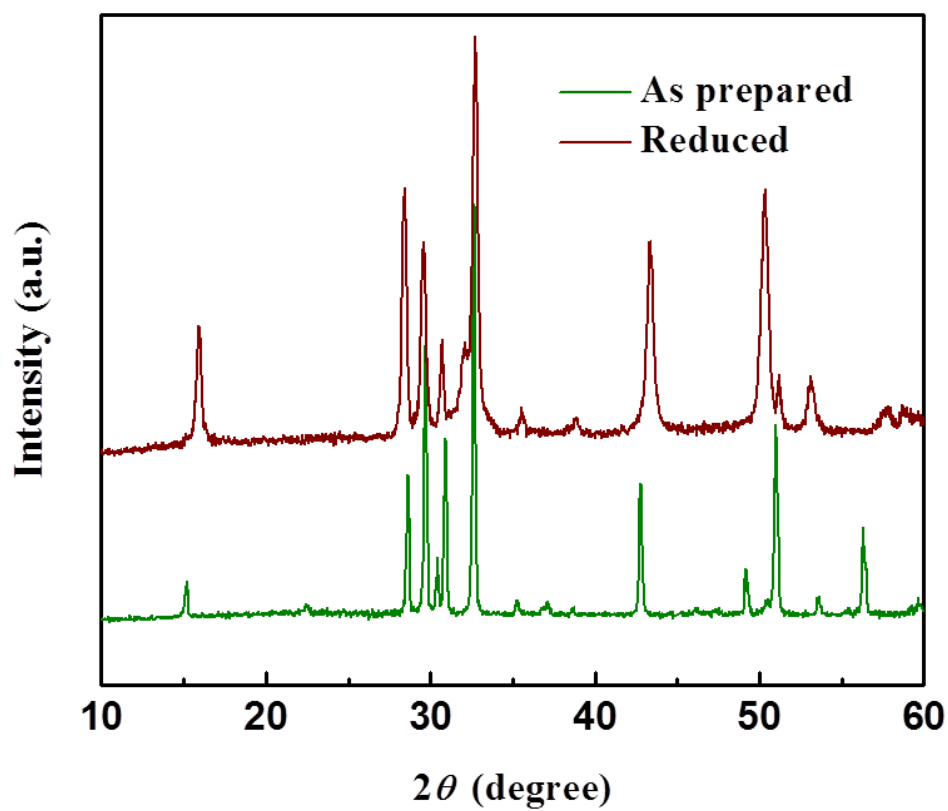


Figure 3. XRD patterns of $\text{YCu}_{0.5}\text{Ti}_{0.5}\text{O}_3$ before (lower) and after (upper) reduction.

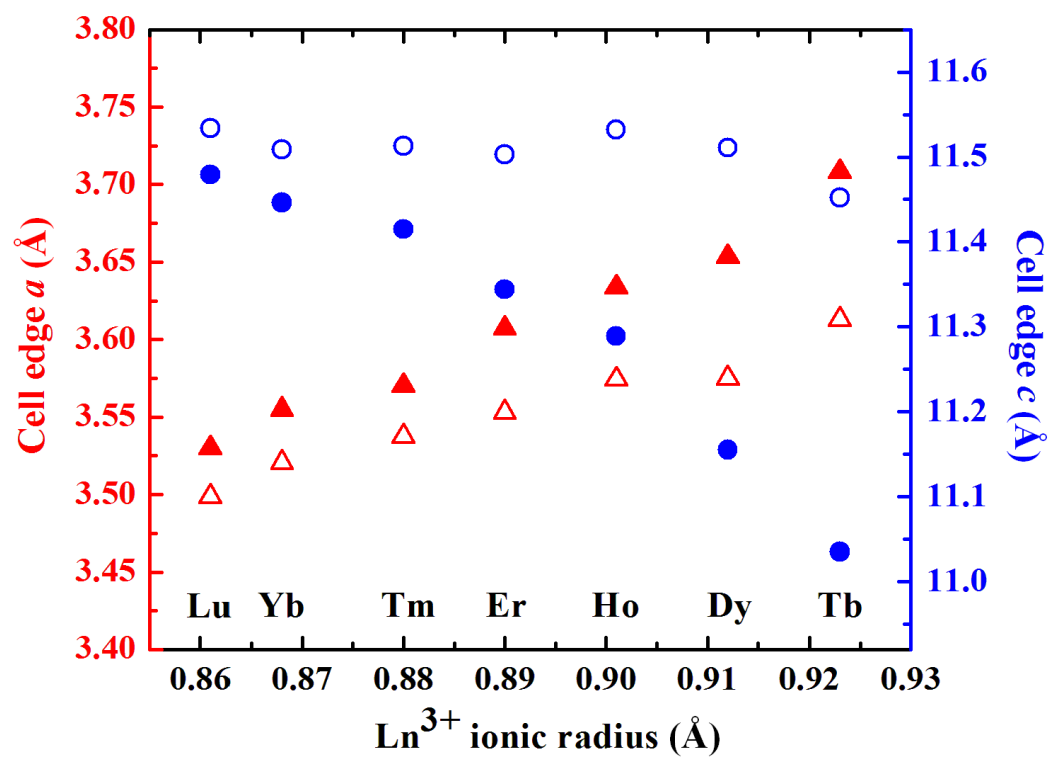


Figure 4. Cell edge of a (triangles) and c (circles) versus ionic radius of R^{3+} ($R = Y, Tb-Lu$) (open points: initial phase; filled points: reduced phase)

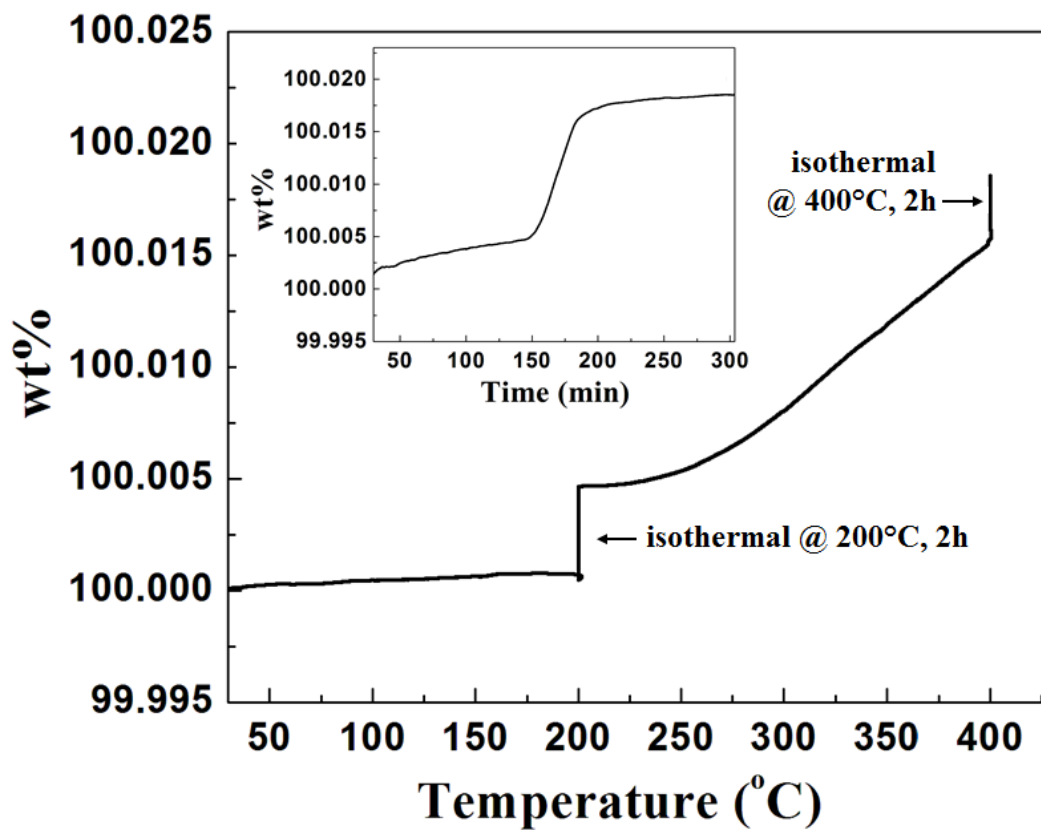


Figure 5. TGA on heating a reduced $\text{YCu}_{0.5}\text{Ti}_{0.5}\text{O}_3$ sample in oxygen. The reduction was carried out at 200 $^{\circ}\text{C}$ in 5% H_2/N_2 and the reoxidation at 200 $^{\circ}\text{C}$ and 400 $^{\circ}\text{C}$ in oxygen, respectively.

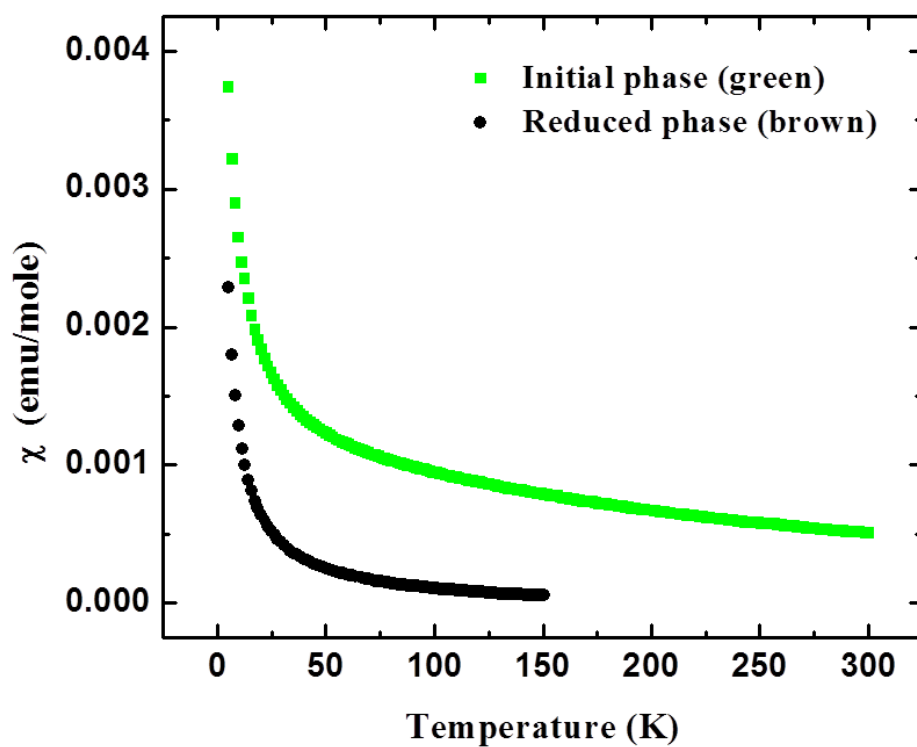


Figure 6. Magnetic susceptibility versus temperature of $\text{YCu}_{0.5}\text{Ti}_{0.5}\text{O}_3$ as prepared (green squares) and reduced (black circles).